

Instability of the fluid pair structure and the freezing density of liquids

Yaakov Rosenfeld

Nuclear Research Center-Negev, P.O. Box 9001, Beer-Sheva 84190, Israel

(Received 22 November 1991)

An instability of the pair-distribution function of the fluid with respect to the diagrammatic iteration loop has been discovered recently [Phys. Rev. A **43**, 6526 (1991)], which correlates well with the freezing density of the soft inverse-power potentials. The present work extends that study to a large variety of pair interactions and establishes the general validity and accuracy of this instability as a semiempirical freezing indicator. Preliminary results for the instability lines for mixtures are also presented that are in qualitative agreement with freezing densities from thermodynamic calculations and from recent experiments on the phase behavior of mixtures of colloids. The stability analysis of the iteration loop is complicated by the need to go beyond linear order.

PACS number(s): 64.70.Dv, 64.10.+h, 05.70.Fh

I. INTRODUCTION

The hypernetted chain [1] (HNC) and other integral equation methods, originating from the diagrammatic low-density expansion in terms of the Mayer f bond, have led to many advances in the theory of liquids [2,3]. The major present-day approximate theories of the structure and thermodynamics of simple liquids interpolate between the standard "ideal-gas," low-density limit and a high-density, "ideal-liquid," limit [4]. The role of the ideal liquid is played by the asymptotic high-density limit of the HNC integral equation (also denoted the "Onsager limit" [4]), which has been proposed as the reference ideal state (replacing the ideal-gas reference state) for developing a systematic theory of the liquid structure [4]. Along this line of development it has been recently discovered [5] that the solution of the HNC integral equation features an instability with respect to the diagrammatic iteration process, which correlates well with the freezing density.

The stability of the solution of the HNC integral equation for the pair-correlation function of the fluid, with respect to its defining diagrammatic iteration loop, was investigated [5] in one, two, and three dimensions ($D=1,2,3$) for the soft ($m/D \leq 4$) inverse-power potentials, $\phi(r)/k_B T = \Gamma r^{-m}$, characterized by a single dimensionless coupling parameter Γ . Two major results emerged from that study [5]: (1) The instability parameters Γ_C correlate well with the freezing parameters Γ_F for the corresponding systems as obtained from computer simulations in $D=3$, as well as with one-phase Lindemann-type structural freezing criteria in $D=1,2,3$; (2) the Onsager limit and the solution of the HNC equation belong to the same basin of attraction with respect to the diagrammatic iterative map. A semiempirical connection was thus established [5] between convergence properties of the diagrammatic low-density Mayer expansion, the asymptotic strong-coupling $\Gamma \rightarrow \infty$ "Onsager" limit of the HNC integral equation, and the freezing density of simple liquids.

There has been a long and not always successful histo-

ry of trying to associate divergences in integral equations with phase transitions, as illustrated by the work of Kozak [6] using the Born-Green-Yvon equation to discuss both freezing and critical exponents. A major impediment to progress along these lines has been the discouraging situation that a given process could yield reasonably accurate freezing parameters for one pair potential while being completely inaccurate for another. The same situation now exists for the density-functional theory of freezing [7]. It is well established that the freezing densities of all simple one-component systems correlate well, e.g., with that of the system of hard spheres with "effective" diameters [8]. "It is not to be expected *a priori* that a similar generality applies to a structural criterion within an approximate theory, as indeed illustrated by previous integral-equation instabilities. Moreover, when working with approximate theories the governing equations are not exact, so that, e.g., the divergence of a particular iteration scheme need not indicate anything about real physics. As illustrated for the density-functional theory of freezing, its accuracy in predicting the fluid-solid transition is strongly potential dependent [7], and may be fortuitous [9]. The results of the HNC instability for the inverse-power potentials, as presented in Ref. [5], are encouraging enough to try and determine what is the real structural information about freezing hidden within these equations, which the iteration process uncovers. Prior to that complicated task (see below), however, and strongly related to it, we have to establish empirically the validity of our instability criterion to *all types* of simple liquids.

The present paper offers an extension of Ref. [5] to a wider class of pair interactions in three dimensions and to mixtures, so that together they cover all available simulation data for simple systems. In the class of inverse-power potentials the results are extended to the important case of hard spheres ($m = \infty$). In order to further elucidate the roles of the steepness and the range of the repulsive interaction, the screened-Coulomb (Yukawa) interaction $\phi(r)/k_B T = (\Gamma/r)e^{-\alpha r}$ is considered for various values of the screening parameter α . With $\alpha=0$ this case corresponds to the one-component plasma, i.e., also the

$m = 1$ inverse-power potential. Accurate simulation results for the freezing of the Yukawa system were obtained only very recently [10]. In order to see the effect of attractive contributions to the potential, the “canonical” Lennard-Jones (12-6) potential $\phi(r) = 4\epsilon[(\sigma/r)^{12} - (\sigma/r)^6]$ is considered down to triple point temperatures. In this class of “realistic” pair potentials, the “EXP-6” potential, $\phi(r) = \epsilon[6/(\alpha-6)]e^{\alpha[1-(r/\sigma)]} - [\alpha/(\alpha-6)](\sigma/r)^6$, with parameters ($\alpha = 13.5$) appropriate for helium and neon is also treated. A general and systematic empirical picture emerges from our study. Preliminary exploration of the “instability” densities for mixtures is presented for binary mixtures of hard spheres and for the binary ionic mixture. The physical understanding of the divergence of the iterative process is complicated by the finding that one must go beyond the standard linear stability analysis.

The brief and general description of the calculations as given in Sec. II intends to be self-contained yet omits many technical details which can be found in Ref. [5]. The results are presented in Sec. III and are discussed in Sec. IV. The Appendix provides the Onsager limits for the Coulomb mixtures and Yukawa potentials which are used as initial seeds for the iterations.

II. DIAGRAMMATIC-EXPANSION ITERATION LOOP AND THE HNC INTEGRAL EQUATION

Diagrammatic analysis [1] reduces the exact calculation of the pair-correlation functions of a classical fluid of particles interacting by the pair potential $\phi(r)$ to the solution of the HNC integral equation for an effective potential $\phi_{\text{eff}}(r) = \phi(r) + B(r)/\beta$, where β is the inverse temperature, $\beta = (k_B T)^{-1}$. The HNC integral equation is composed of the Ornstein-Zernike relation between the direct correlation function $c(r)$ and the radial distribution function $g(r) \equiv h(r) - 1$ and the HNC closure. Recalling the screening potential, $H(r) = h(r) - c(r)$, the Ornstein-Zernike relation $\tilde{h}(k) = \tilde{c}(k) + \rho \tilde{h}(k) \tilde{c}(k)$ has the following k -space form:

$$\tilde{H}(k) = \rho \tilde{c}^2(k) / [1 - \rho \tilde{c}(k)]. \quad (1)$$

The HNC closure for a potential $\phi_{\text{eff}}(r)$ is

$$c(r) = \exp[-\beta \phi_{\text{eff}}(r) + H(r)] - 1 - H(r), \quad (2)$$

where ρ is the number density and tildes denote Fourier transforms. Upon inserting Eq. (1) into Eq. (2) one obtains the HNC integral equation. The bridge function $B(r)$ may be expanded in diagrams with the $h(r)$ bond [1,2]. The HNC approximation, i.e., the assumption $B(r) = 0$, consists of the solution of the HNC equation for $\phi_{\text{eff}}(r) = \phi(r)$, and is the starting point for a systematic diagrammatic expansion for $B(r)$.

The diagrammatic expansion corresponding to the HNC approximation is obtained by the following iteration loop [1]: starting with the Mayer f -bond seed $c_{\text{Mayer}}(r) = f(r) \equiv \exp[-\beta \phi(r)] - 1$ in Eq. (1), the resulting $H(r)$ is fed into Eq. (2), which yields the first iteration for $c(r)$, which is then fed again into Eq. (1), and so on. The numerical solution of the HNC integral equation is achieved, however, by “relaxation” and “Newton-

Raphson” methods [11].

The stability of the solution of the HNC equation is checked by generating numerically the diagrammatic iteration loop (1) and (2). Given the pair potential, the temperature, and the density (and the composition for a mixture), then two types of calculations were performed, which differ only in the initial seed, $c_0(r)$, to be fed into Eq. (1) instead of $c_{\text{Mayer}}(r)$.

(i) When available, use the asymptotic limit of the solution of the HNC equation (the “ideal liquid”), $c_0(r) = c_{\text{HNC}}^{\infty}(r)$, as the initial seed in the iteration loop (1) and (2).

(ii) Obtain first a solution (with some prescribed high accuracy) to the HNC equation using a standard numerical method. Use this solution as the initial seed in the iteration loop (1) and (2).

The computational setup, as governed by a numerical fast Fourier transform (FFT) procedure, is completely characterized by the mesh points for describing the correlation functions [5,11], $\{h(r_i); r_i = i\Delta r; i = 1, \dots, N; N = 2^M\}$, $\{\tilde{h}(k_i); k_i = i\Delta k; \Delta k = \pi/N\Delta r\}$. The two independent parameters M and Δr were widely varied, and it was found that the results are very *robust* with respect to the mesh of points. A good compromise turned out to be $N = 128$, $\Delta r = 0.1$, with r measured in units of the Wigner-Seitz radius a_{WS} given by $\rho(a_{\text{WS}})^3 = 3/4\pi$. The results for the “critical” densities show little sensitivity to large (up to 16-fold) variations in N and Δr . The mesh size N defines the dimensionality of the iteration map. See details in Ref. [5].

At any given iteration step; we found it useful [5] to define and monitor the following quantities: at the “series” part of the loop, i.e., Eq. (1), define $h_S(r)$ as the inverse Fourier transform of $\tilde{h}_S(k) \equiv \tilde{c}(k) / [1 - \rho \tilde{c}(k)]$, and in the “parallel” part of the loop, Eq. (2), define $h_P(r) \equiv \exp[-\beta \phi(r) + H(r)] - 1$. At any given iteration step define u_p and u_s , the potential energy integrals as obtained from $u = (\rho/2) \int [h(r) + 1] \beta \phi(r) d\mathbf{r}$, upon using $h_p(r)$ and $h_s(r)$, respectively. For the one-component plasma use $h(r)$ instead of $h(r) + 1$ in the integral. The corresponding expressions for the HNC free-energy integrals [4] were similarly monitored [5]. The extension of these definitions, equations, and numerical procedures to mixtures is straightforward [12].

III. RESULTS

The first purpose of the present study was to establish empirically the general properties of the iterations near their instability and, in particular, to find out whether the correlations between the instability densities and the freezing densities are indeed general. Such an accidental correlation for a limited class of potentials may cast doubt on the physical meaning of the instability beyond its mathematical interest. This is not the case with the HNC instability since the main general results of the present study are in agreement with those of Ref. [5], which are thus extended to a large variety of quite disparate potentials and to mixtures.

The Onsager limit and the solution to the HNC equation belong to the same basin of attraction with respect to

the diagrammatic iterative map. In other words, whenever both calculations of type (i) and type (ii) above are available (Yukawa, Coulomb, and see Ref. [5]) then their end results are identical.

For all $\rho < \rho_C$ the calculations always converge to the solution of the HNC integral equation. As the iteration number increases for $\rho < \rho_C$, the energy integral u_s is generally monotonically decreasing while the energy integral u_p is monotonically increasing, and eventually they become equal for the HNC solution.

For $\rho > \rho_C$ starting from the Onsager seed the diagrammatic iteration loop rapidly converges to a limit cycle composed of several functions, the number of which depends on the type of potential. In the vicinity of ρ_C , however, for $\rho > \rho_C$, the iterations *always* begin to exhibit a three-function cycle pattern. These three-function patterns gradually change as the iterations continue. Considering the “time series” $E(t)$, i.e., the energy vs iteration number, then $E(t)$ seems to converge for $\rho > \rho_C$ to a pattern $E^{(\infty)}(t)$ that can be expressed by the following *universal* form:

$$E(t \gg 1) = E^{(\infty)}(t) = F[t - L(t \bmod 3)]. \quad (3)$$

The function $F(t)$ is periodic with period T . The number of functions in the limit cycle, N_E , i.e., the number of distinct energy levels in the pattern $E^{(\infty)}(t)$, satisfies $N_E \leq L$.

The cases $m = 1$ in two and three dimensions ($D = 2, 3$) are the only cases studied before [5] to feature $L = 3$ (i.e., a three-function limit cycle) in the immediate vicinity of Γ_C . This feature holds also for the Yukawa potential provided that the screening is weak, $\alpha \leq 2.3$. For binary ionic mixtures this feature of a three-function limit cycle holds only for certain compositions. The composition dependence of the parameters, e.g., N_E and L , requires further study

In view of this universal occurrence of the “critical” densities for the stability of the solution of the HNC equation, the main question is its correlation with the freezing densities for the corresponding systems. Combining the present results with those of Ref. [5], a systematic picture is emerging which will now be described starting with the hard spheres and other inverse-power potentials, $\phi(r) = \epsilon(\sigma/r)^m$. For the hard spheres, $m = \infty$, we find the “critical” packing fraction $\eta_C = \pi\rho_C\sigma^3/6 = 0.445 \pm 0.001$. The results for the inverse-power potentials are summarized in Table I and in Fig. 1. The reduced density $x = (\epsilon/k_B T)^{3/m} \rho \sigma^3$ is related to the coupling parameter Γ by $\Gamma = (4\pi x/3)^{m/3}$. The ratio between the “critical” density to the freezing density, x_C/x_F , increases monotonically when the potential becomes less steep and of longer range; e.g., it is 0.90 for $m = \infty$, 1.01 for $m = 9$, and 1.09 for $m = 4$. The results for the Lennard-Jones (12-6) system, given in Table II, are generally consistent with those for the inverse-power potential with an effective power which increases from $m = 12$ as the temperature is lowered along the freezing line. The effective power can be defined by the logarithmic derivative, $m_{\text{eff}} = 3(\partial \ln T^* / \partial \ln \rho^*)$, along the freezing line, which gives $m_{\text{eff}} = m$ for the inverse-power potentials. Similarly consistent results for the exp-6 poten-

TABLE I. Freezing and melting densities of the inverse-power potentials, $\phi(r) = \epsilon(\sigma/r)^m$. The simulation results [13,14] for the reduced freezing (x_F) and melting (x_M) densities, $x = (\epsilon/k_B T)^{3/m} \rho \sigma^3$, compared with the HNC instability parameters (x_C).

m	x_M	x_F	x_C	x_C/x_F
∞	1.041	0.943	0.850	0.90
12	1.193	1.141	1.084	0.95
9	1.373	1.333	1.346	1.01
6	2.21	2.17	2.27	1.04
4	4.57	4.53	4.94	1.09
1	1.24×10^6	1.24×10^6	1.65×10^6	1.33

tial are given in Table III. The results for the Yukawa potential are presented in Table IV and in Figs. 2 and 3. Note that Fig. 1 is constructed for comparison with Fig. 2. The HNC instability is thus the first freezing indicator of its type, which indicates reasonably well the freezing density for any potential.

The exploration of the “critical” instability densities for mixtures is technically the same as for the one-component systems. The binary mixture is composed of two types of particles of relative concentrations $x_1, x_2 = 1 - x_1$, interacting via the potentials $\phi_{ij}(r)$ ($i, j = 1, 2$). The binary hard-sphere mixture, composed of hard spheres of radii R_i ($i = 1, 2$), is completely characterized by x_1 , the ratio R_1/R_2 and the total packing fraction $\eta = (\pi\rho R_1^3 + \pi\rho R_2^3)/6$, where $\rho = (N_1 + N_2)/V$ is the total number density. The results for binary mixtures of hard spheres are presented in Fig. 4. The two-component plasma is composed of point ions of charges Q_1 and Q_2 , in a uniform neutralizing background of electrons. The pair interaction is the Coulomb potential $\beta\phi_{i,j}(r) = \Gamma Q_i Q_j / r$ with r measured in units of the total Wigner-Seitz radius, a_{WS} , given by $4\pi a_{\text{WS}}^3/3 = \rho$. Following the ion-sphere model, the mixture excess free energy can be approximated by the one-

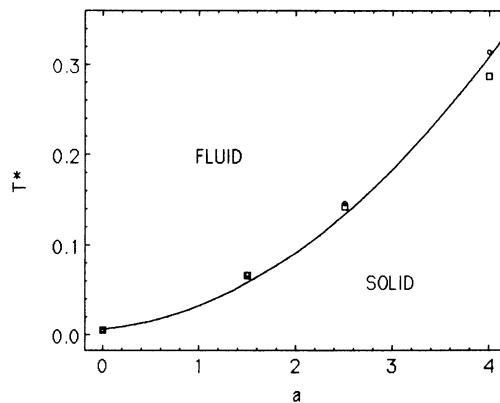


FIG. 1. Freezing and melting densities of the inverse-power potentials, $\beta\phi(r) = \Gamma r^{-m}$. The simulation results [13] for the freezing (circles) and melting (squares) parameters in the range $1 \leq m \leq 9$ are compared with the HNC instability parameters (full line). To compare with the results for the Yukawa system we plot $T^* = e^a/\Gamma$ vs $a = (m - 1)/2$.

TABLE II. Freezing line for the Lennard-Jones potential, $\phi(r)=4\epsilon[(\sigma/r)^{12}-(\sigma/r)^6]$. The reduced freezing density $\rho_F^*=\rho_F\sigma^3$ as function of the reduced temperature $T^*=kT/\epsilon$ from the simulations [13,15], compared with the HNC instability density $\rho_C^*=\rho_C\sigma^3$.

T^*	ρ_F^*	ρ_C^*	ρ_C^*/ρ_F^*
100	2.601	2.48±0.01	0.953
10	1.50	1.425±0.005	0.950
5	1.279	1.205±0.005	0.942
2.74	1.113	1.065±0.002	0.957
1.35	0.964	0.913±0.002	0.947
1.15	0.936	0.883±0.003	0.943
0.75	0.875	0.805±0.005	0.920

TABLE III. Freezing line for the exp-6 potential, $\phi(r)=\epsilon\{[6/(\alpha-6)]e^{\alpha(1-r/\sigma)}-[1/(\alpha-6)](\sigma/r)^6\}$, $\alpha=13.5$. The reduced freezing density $\rho_F^*=\rho_F\sigma^3$ as function of the reduced temperature $T^*=kT/\epsilon$ from a theoretical calculation [13,16] using lattice dynamics and variational fluid theory, compared with the HNC instability density $\rho_C^*=\rho_C\sigma^3$.

T^*	ρ_F^*	ρ_C^*	ρ_C^*/ρ_F^*
29.41	3.71	3.95±0.05	1.065
10	2.48	2.55±0.05	1.03
3	1.73	1.75±0.05	1.01

TABLE IV. Freezing line for the Yukawa potential, $\beta\phi(r)=\Gamma e^{ar}/r$, from molecular dynamics [10] compared with the HNC instability parameters. The parameters used in Ref. [10] are related to the potential parameters by $T^*=e^a/\Gamma/(3/4\pi)^{1/3}$, $a=\alpha/(3/4\pi)^{1/3}$.

Molecular dynamics		HNC instability	
T^*	a	T^*	a
0.0089±0.0004	0	0.0081	0
0.079±0.004	2.95	0.0055	2.418
		0.104	3.627
0.115±0.005	3.86	0.115	3.86
		0.166	4.836
0.198±0.008	5.38	0.196	5.38
		0.293	6.770
0.284±0.008	6.87		
Γ	α	Γ	α
180±10	0	198±2	0
		329±2	1.5
390±20	1.83	413±2	1.83
		583±3	2.25
664±30	2.39	662±3	2.39
		1225±5	3
1760±70	3.34	1775±10	3.34
		4800±10	4.2
5460±150	4.26		

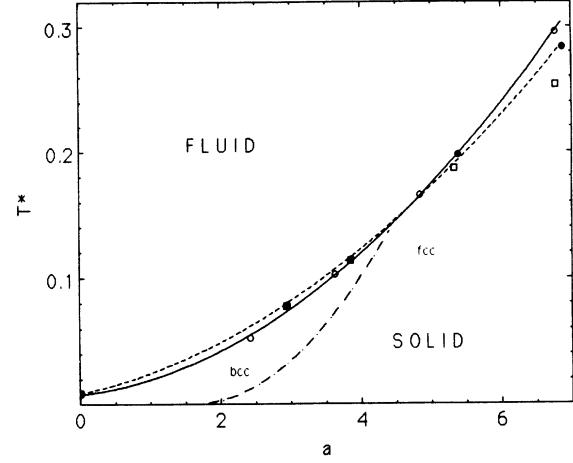


FIG. 2. Freezing line for the Yukawa potential, $\beta\phi(r)=\Gamma e^{ar}/r$, from molecular dynamics [10] (open circles and full line) compared with the HNC instability parameters (full circles and broken line). Also shown are the melting line (squares) and the bcc-fcc transition line for the solid [10]. The parameters used in Ref. [10] are related to the potential parameters by $T^*=e^a/\Gamma/(3/4\pi)^{1/3}$, $a=\alpha/(3/4\pi)^{1/3}$.

component system with an effective coupling given by [17] $\Gamma_{\text{eff}}=\Gamma\langle Q \rangle^{1/3}\langle Q^{5/3} \rangle$, where $\langle Q^i \rangle=x_1Q_1^i+x_2Q_2^i$. To this first approximation it is thus expected [17] that the freezing of the binary ionic mixture is given by the freezing of the one-component system ($\Gamma_{\text{eff}})_F=180$. We thus define $\Gamma^*=198/(\langle Q \rangle^{1/3}\langle Q^{5/3} \rangle)$, which is the expected value of $\Gamma_{C,\text{mix}}$ in that approximation. The results for the ratio $G=\Gamma_{C,\text{mix}}/\Gamma^*$ between the calculated instability coupling parameter and that expected on the basis of ion-sphere scaling for the binary ionic mixture are given in Fig. 5. Let $Z=Q_1/Q_2$ be the charge ratio ($Q_1 \geq Q_2$); then the freezing line at constant charge density, as predicted by the scaling approximation above, is given by $T/T_2=1+(Z^{5/3}-1)x_1$, where T_2 is the freezing temperature for the one-component system of charges Q_2 , i.e., $x_1=0$. The instability line at constant charge density is given by (see Figs. 6 and 7) $T/T_2=[1+(Z^{5/3}-1)x_1]/G$, where now T_2 is the insta-

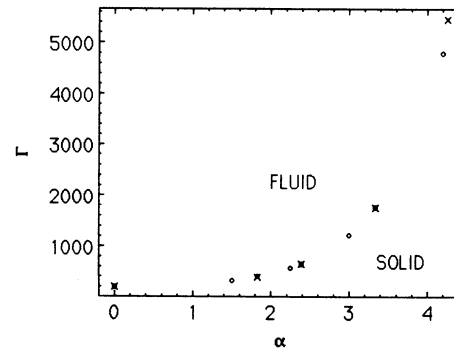


FIG. 3. Freezing line for the Yukawa potential, $\beta\phi(r)=\Gamma e^{ar}/r$, from molecular dynamics [10] (\times) compared with the HNC instability parameters (open circles). See Table IV.

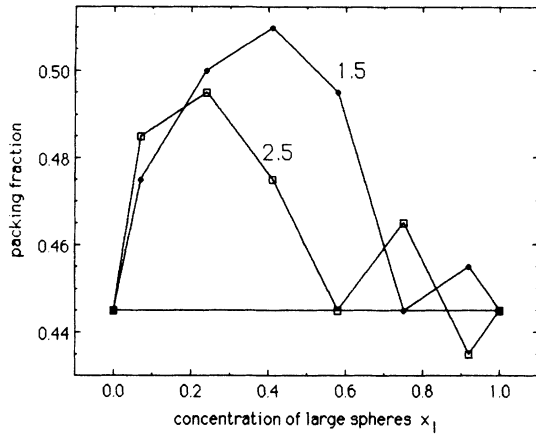


FIG. 4. "Critical" (HNC instability) parameters as a function of the total packing fraction of the spheres and the concentration of the large spheres, for binary hard-sphere mixtures with diameter ratios $\sigma_1/\sigma_2=1.5$ (circles) and $\sigma_1/\sigma_2=2.5$ (squares). The lines serve as a guide to the eye.

bility temperature for the one-component system of charges Q_2 , i.e., $x_1=0$.

IV. DISCUSSION

The present results for a large variety of pair interactions ("hard spheres," "Yukawa," "Lennard-Jones (12-6)," and "exp-6" potentials), together with the results of Ref. [5] for the soft inverse-power potentials, enable finding a general systematic behavior. The ratio between the "critical" ("instability") densities, ρ_C , and the freezing densities, ρ_F , increases monotonically as the steepness of the interaction decreases. It varies between the extreme values of $\rho_C/\rho_F=0.9$ for hard spheres and $\rho_C/\rho_F=1.3$ for the Coulomb potential. Since the di-

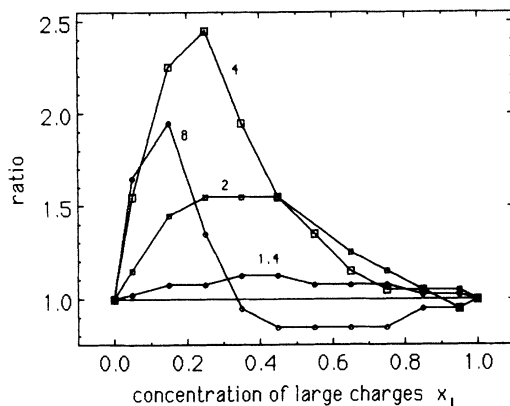


FIG. 5. "Critical" (HNC instability) parameters for the two-component plasma, composed of two types of ions in a compensating rigid background of electrons. Results for charge ratios $Q_1/Q_2=1.4, 2, 4, 8$ are given as a function of the concentration of the large charges and the coupling parameter given in terms of the "ratio" (see the text) between the calculated instability coupling parameter and that expected on the basis of ion-sphere scaling for the binary ionic mixture.

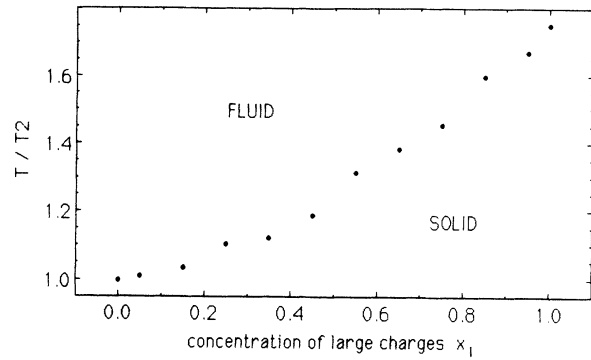


FIG. 6. The instability temperature at constant charge density, T/T_2 , for a binary ionic mixture with charge ratio $Q_1/Q_2=1.4$, as a function of the concentration of the larger charges, x_1 . T_2 is the instability temperature for the one-component system of charges Q_2 , i.e., at $x_1=0$.

agrammatic iteration does not give information about the solid, ρ_C cannot be equal to ρ_F and thus represents a structural (not thermodynamic) freezing indicator. The relevant scale for evaluating the correlations between the "instability" densities ρ_C and the freezing ρ_F for not very soft potentials is the density change upon freezing. On this scale, the "instability" densities ρ_C correlate with the freezing parameters ρ_F for the corresponding systems, better than any other Lindemann-type freezing indicator. In this context the gross empirical correlation between $\rho_C/\rho_F=1$ and crossover between the fcc and bcc relative stability of the coexisting crystal structure, as found for both the inverse-power potentials [5] and for the Yukawa system, are interesting. The accurate determination of the freezing density for the one-component plasma is difficult for any theory, and the 30% difference between ρ_C and ρ_F corresponding to the difference between $\Gamma=200$ and 180, respectively, is on the scale of the uncertainty for ρ_F .

Accurate freezing results for mixtures are required before a detailed comparison with the instability densities can be performed. Pending the availability of the ap-

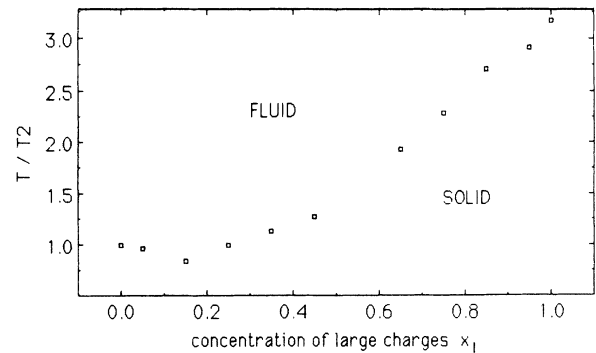


FIG. 7. The instability temperature at constant charge density, T/T_2 , for a binary ionic mixture with charge ratio $Q_1/Q_2=2$, as a function of the concentration of the larger charges, x_1 . T_2 is the instability temperature for the one-component system of charges Q_2 , i.e., at $x_1=0$.

appropriate freezing simulation data for mixtures, it is interesting to observe that the hard-sphere results of Fig. 4 are in qualitative agreement with the results in Ref. [18], based on density-functional calculations, and the results of Ref. [19]. The qualitative similarity between our results for hard spheres and point ions, Figs. 4 and 5, is also interesting. Both show that the fluid phase is stable to a higher density in the binary mixture than in the monodisperse system, and that the maximum fluid freezing density occurs in mixtures rich in small particles, with the proportion of small spheres increasing sharply with increasing diameter ratio. The density of the binary-mixture fluid increases from that for the monodisperse case up to a maximum value for diameter ratios about 1.5 and then decreases. These results for the instability densities for mixtures are also in qualitative agreement with recent experiments, using light scattering and scanning electron microscopy, on the phase behavior of mixtures of colloidal hard spheres [20]. Qualitatively similar phase behavior has also been observed [21] in binary suspensions of charged colloids where at intermediate compositions the liquid phase remained stable up to a higher number density in the mixture than in the individual pure suspensions. Figure 6 favors the carbon-oxygen phase diagram of Ref. [22] over that of Ref. [23], while Fig. 7 predicts an “azeotropic” or “eutectic” phase diagram for the helium-hydrogen binary ionic mixture.

The “instability” parameters ρ_C represent perhaps an upper bound for the radius of convergence of the diagrammatic, small- ρ , Mayer expansion of the pair-correlation functions. This seems to be a reasonable conclusion if we recall that the diagrammatic expansion as described by van Leeuwen *et al.* [1] begins with the HNC approximation, and its failure to converge may be indicative for the full expansion. It should be remembered, however, that the omitted bridge diagrams could make the true radius of convergence either larger or smaller. Moreover, since the HNC approximation is only the first step in the systematic diagrammatic expansion [1], its instability need not indicate anything about real physics. The correlation between ρ_C and freezing however, provides strong indication that there is real physics behind it. It demonstrates that the diagrammatic iteration process, which eventually builds up the fluid correlation functions, also contains information regarding the stability of this structure. The question of what is the specific, local, or integral property of a given pair structure, which makes it unstable with respect to the iteration loop, is still open. The structure factors $S(k) = 1 + \rho \tilde{h}(k)$ as obtained from the solution of the HNC equation at the instability density for a large variety of potentials are displayed together in Fig. 8. These $S(k)$ exhibit the expected similarity as featured by the Hansen-Verlet “rule” [13,15] concerning the height of the first peak of the structure factor. The solutions do not exhibit, however, any drastic change across the instability densities, except of course the stability property with respect to the iteration loop. The standard stability analysis [24] of the diagrammatic iterative map may eventually lead to an answer, giving perhaps a different quantitative structural definition for “effective packing.” It should be em-

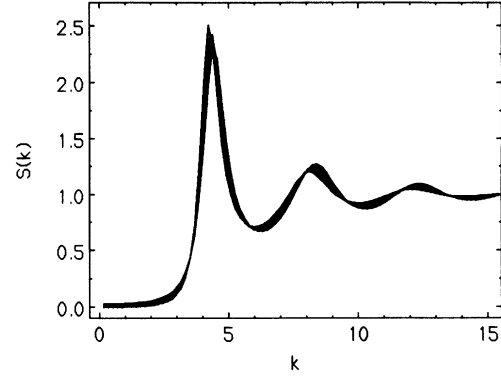


FIG. 8. The structure factors $S(k)$ as obtained from the solution of the HNC equation at the “critical” (instability) density for all soft inverse-power potentials and all Yukawa potentials considered in Tables I and IV. The “wave vector” k is in units of the inverse of the Wigner-Seitz radius.

phasized, however, that the real eigenvalue spectrum of the Floquet matrix [24] (corresponding to the linearization of the iteration map) for the iterations near the HNC solution does not show any qualitative change across the “critical” density. Our extensive effort with the standard linear-stability analysis only indicated the need to go beyond the linear analysis. Considering the multidimensionality of the iterative map ($D \cong N$) makes the task very (if not prohibitively) complicated. The relation of the three-function limit cycles to Sharkovsky’s theorem [25], if it exists, also remains to be clarified.

The HNC integral equation provides an accurate description of the fluid pair structure and features an instability which provides a good estimate of the freezing density. Considering the asymptotic (“Onsager”) limit of the solutions to the HNC equation the “ideal liquid,” it then provides, as the initial seed for the diagrammatic iteration loop, both the structure of the fluid and an indication of its instability. The HNC instability, as a semi-empirical freezing indicator, is at present the only one of its kind to be nearly equally accurate for *all* potentials. Accurate simulation results for the freezing of fluid mixtures are still needed in order to evaluate the instability lines for mixtures.

APPENDIX: ASYMPTOTIC DIRECT CORRELATION FUNCTIONS (REF. [4])

(a) The asymptotic (Onsager) direct correlation function for the two-component plasma, composed of point ions of charges Q_1 and Q_2 , has the form $(i, j = 2) c_{\text{HNC},ij}^\infty(r) = -\Gamma \Psi_{ij}(r)$, where $\Psi_{ij}(r)$ is given by the electrostatic interaction between the two charges Q_1 and Q_2 at distance r , when each is uniformly smeared in the volume of a sphere of radius R_1 and R_2 , respectively. The distance r is measured in units of the total Wigner-Seitz radius, a_{WS} , and $R_1^3 = Q_1 / \langle Q \rangle$ and $R_2^3 = Q_2 / \langle Q \rangle$, where $\langle Q \rangle = x_1 Q_1 + x_2 Q_2$. Let $R_1 > R_2$ and define the quantities $X_L = R_1 - R_2$, $X_R = R_1 + R_2$, $V_1 = 4\pi R_1^3 / 3$, $V_2 = 4\pi R_2^3 / 3$, $A_Z = 2(\pi/12)(X_R - X_L)^3$, $A_1 = -3(\pi/12)(X_R X_L)^2$, $A_2 = 2(\pi/12)X_R(X_R^2 + 3X_L^2)$, and $A_3 = -3(\pi/12)(X_R^2 + X_L^2)$; then the function $\Psi_{12}(r)$ is given by the following expressions.

$$\Psi_{12}(r) = \begin{cases} Q_1 Q_2 (4\pi/V_1/V_2) [A_Z r^2/3 + A_Z (X_L^2 - r^2)/2 + A_1 (X_R - X_L) \\ \quad + A_2 (X_R^2 - X_L^2)/2 + A_3 (X_R^3 - X_L^3)/3 + (\pi/12)(X_R^5 - X_L^5)/5] & \text{for } r < X_L \\ Q_1 Q_2 (4\pi/V_1/V_2) [A_Z X_L^3/3/r + A_1 (r^2 - X_L^2)/2/r \\ \quad + A_2 (r^3 - X_L^3)/3/r + A_3 (r^4 - X_L^4)/4/r + (\pi/12)(r^6 - X_L^6)/6/r + A_1 (X_R - r) \\ \quad + A_2 (X_R^2 - r^2)/2 + A_3 (X_R^3 - r^3)/3 + (\pi/12)(X_R^5 - r^5)/5] & \text{for } X_L < r < X_R \\ Q_1 Q_2 / r & \text{for } r > X_R \end{cases}$$

(b) The asymptotic (Onsager) direct correlation function for the Yukawa potential $\beta\phi_{\text{Yuk}}(r) = \Gamma e^{-\alpha r}/r$ has the form $c_{\text{HNC}}^\infty(r) = -\Gamma\Psi(\alpha, r)$, where $\Psi(\alpha, r)$ is given by the Yukawa interaction between two "charges" q_{eff} at distance r , each uniformly smeared in the volume of a sphere of unit radius. The distance r is measured in units of the Wigner-Seitz radius, a_{WS} . Define $S_D = e^\alpha(\alpha - 1) + e^{-\alpha}(\alpha + 1)$, then $q_{\text{eff}} = 2/3/(S_D/\alpha^3)$. Define further $A = 3q_{\text{eff}}^2/\alpha^2$, $B = 1.5A(1 - \alpha^2)/\alpha^2$, $V = -3q_{\text{eff}}(1 + \alpha)/\alpha^2/e^\alpha$. The function $\Psi(\alpha, r)$ is given by

$$\Psi(\alpha, r) = A + Br/2 + Ar^3/16 + V(1 - e^{-\alpha r})/\alpha/r \\ + (V^2/2/\alpha/\alpha/r)[1 - \cosh(\alpha r)] \quad \text{for } r < 2$$

and

$$\Psi(\alpha, r) = e^{-\alpha r}/r \quad \text{for } r > 2.$$

This representation for the Yukawa asymptotic limit function is based on an analysis [26] of the Onsager given in Appendix B of Ref. [27], which was derived as a limit of the mean-spherical-approximation direct correlation function.

(c) The asymptotic (Onsager) direct correlation functions $C_{nl}^\infty(r)$, for the binary hard-sphere mixture, is proportional to the overlap volume of two spheres of radii R_n, R_l and separation r , $\Omega_{nl}(r)$. We do not know *a priori* the coefficient $c_{nl}^\infty(r=0)$ for the HNC equation.

-
- [1] J. M. J. van Leeuwen, J. Groeneveld, and J. deBoer, *Physica (Utrecht)* **25**, 792 (1959); T. Morita and K. Hiroike, *Prog. Theor. Phys. (Jpn.)* **23**, 1003 (1960).
- [2] Y. Rosenfeld and N. W. Ashcroft, *Phys. Rev. A* **20**, 1208 (1979). This paper contains an appendix discussing the diagrammatic iteration loop for the Coulomb potential.
- [3] (a) J. Barker and D. Henderson, *Rev. Mod. Phys.* **48**, 587 (1976); (b) J. P. Hansen and I. R. McDonald, *Theory of Simple Liquids*, 2nd ed. (Academic, London, 1986); (c) J. Talbot, J. L. Lebowitz, E. M. Weisman, D. Levesque, and J. J. Weis, *J. Chem. Phys.* **85**, 2187 (1986); (d) see also the recent review, R. Evans, in *Liquids at Interfaces*, Proceedings of the Les Houches Summer School of Theoretical Physics, Session 48, edited by J. Chavrolin, J. F. Joanny, and J. Zinn-Justin (Elsevier, Amsterdam, 1989).
- [4] Y. Rosenfeld, *Phys. Rev. A* **32**, 1834 (1985); **33**, 2025 (1986); **35**, 938 (1987); **37**, 3403 (1988); *Phys. Rev. Lett.* **63**, 980 (1989).
- [5] Y. Rosenfeld, *Phys. Rev. A* **43**, 6526 (1991).
- [6] See, for example, the review by John Kozak, *Nonlinear Problems in the Theory of Phase Transitions*, Vol. XL of *Advances in Chemical Physics*, edited by I. Prigogine and S. A. Rice (Wiley, New York, 1979).
- [7] A. de Kuijper, W. L. Vos, J. L. Barrat, J. P. Hansen, and J. A. Schouten, *J. Chem. Phys.* **93**, 2692 (1990).
- [8] Structural, Lindemann-type freezing criteria are reviewed by Y. Rosenfeld, *Phys. Rev. A* **24**, 2805 (1981).
- [9] (a) W. A. Curtin, *J. Chem. Phys.* **88**, 7050 (1988); (b) Y. Rosenfeld, *Phys. Rev. Lett.* **63**, 980 (1989); (c) Y. Rosenfeld, D. Levesque, and J. J. Weis, *J. Chem. Phys.* **92**, 6818 (1990); (d) S. J. Smithline and Y. Rosenfeld, *Phys. Rev. A* **42**, 2434 (1990); (e) Y. Rosenfeld, *ibid.* **43**, 5424 (1991).
- [10] E. J. Meijer and D. Frenkel, *J. Chem. Phys.* **94**, 2269 (1991).
- [11] See, for example, K. N. Ng, *J. Chem. Phys.* **61**, 2680 (1974); M. J. Gillan, *Mol. Phys.* **38**, 1781 (1979); G. M. Abernethy and M. J. Gillan, *ibid.* **39**, 839 (1980); S. Labik, A. Malijevsky, and P. Vonka, *ibid.* **56**, 709 (1985).
- [12] Details of a HNC program for mixtures are given by S. W. Rick and A. D. J. Haymet, *J. Chem. Phys.* **90**, 1188 (1989).
- [13] Reviews of computer-simulation freezing data are given by W. G. Hoover and M. Ross, *Contemp. Phys.* **12**, 339 (1971); S. M. Stishov, *Usp. Fiz. Nauk* **114**, 3 (1974) [*Sov. Phys. Usp.* **17**, 625 (1975)]; **154**, 93 (1988) [**31**, 52 (1988)].
- [14] B. J. Alder, W. G. Hoover, and D. A. Young, *J. Chem. Phys.* **49**, 3688 (1968); W. G. Hoover and F. Ree, *ibid.* **49**, 3609 (1968).
- [15] J. P. Hansen, *Phys. Rev. A* **2**, 221 (1970); J. P. Hansen and L. Verlet, *Phys. Rev.* **184**, 151 (1969).
- [16] M. Ross, *Phys. Rev. A* **8**, 1466 (1973); See also W. L. Voss, J. A. Schouten, D. A. Young, and M. Ross, *J. Chem. Phys.* **94**, 3835 (1991).
- [17] M. Bous and J. P. Hansen, *Phys. Rep.* **59**, 1 (1980).
- [18] A. R. Denton and N. W. Ashcroft, *Phys. Rev. A* **42**, 7312 (1990), Fig. 4.
- [19] P. Bartlett, *J. Phys. Condens. Matter* **2**, 4979 (1990).
- [20] P. Bartlett, R. H. Ottewill, and P. N. Pusey, *J. Chem. Phys.* **93**, 1299 (1990).
- [21] S. Hachisu, A. Kose, Y. Kobayashi, and K. Takano, *J. Coll. Interface Sci.* **55**, 499 (1976); H. M. Lindsay and P. M. Chaikin, *J. Chem. Phys.* **76**, 3774 (1982); W. Y. Shih, W. Shih, and I. A. Aksay, *ibid.* **90**, 4506 (1989).
- [22] J. L. Barrat, J. P. Hansen, and R. Mochkovich, *Astron. Astrophys.* **199**, L15 (1988).

- [23] S. Ichimaru, H. Iyetomi, and S. Ogata, *Astrophys. J.* **334**, L17 (1988).
- [24] See, for example, P. Bergè, Y. Pomeau, and C. Vidal, *Order within Chaos* (Wiley, Paris, 1986).
- [25] SR. Z. Sagdeev, D. A. Usikov, and G. M. Zaslavsky, *Non-linear Physics: From the Pendulum to Turbulence and Chaos* (Harwood, Chur, Switzerland, 1988), Chap. 3.
- [26] Y. Rosenfeld and L. Blum (unpublished).
- [27] J. Stein, D. Shalitin, and Y. Rosenfeld, *Phys. Rev. A* **37**, 4854 (1988).